Optimal control theory for continuous-variable quantum gates

Rebing Wu, Raj Chakrabarti, and Herschel Rabitz
Department of Chemistry, Princeton University, Princeton, New Jersey 08544, USA
(Received 15 August 2007; revised manuscript received 10 January 2008; published 1 May 2008)

The methodology of optimal control theory is applied to the problem of implementing quantum gates in continuous-variable (CV) systems with quadratic Hamiltonians. We demonstrate that it is possible to define a fidelity measure for CV gate optimization that is devoid of traps, such that the search for optimal control fields using local algorithms will not be hindered. The optimal control of several quantum computing gates, as well as that of algorithms composed of these primitives, is investigated using several typical physical models and compared for discrete-variable and continuous-variable quantum systems. Numerical simulations indicate that the optimization of generic CV quantum gates is inherently more expensive than that of generic discrete variable quantum gates, but can be routinely achieved for all the major classes of computing primitives. The exact-time controllability of CV systems, hitherto largely ignored in the design of information processing models, is shown to play an important role in determining the maximal achievable gate fidelity. Moreover, the ability to control interactions between qunits can be exploited to delimit the total control fluence. Future experimental model systems should carefully tune these parameters so as to enable the implementation of CV quantum information processing with optimal fidelity.

DOI: 10.1103/PhysRevA.77.052303 PACS number(s): 03.67.Lx, 02.30.Yy, 02.70.−c

I. INTRODUCTION

The optimal control of quantum dynamical systems has become a subject of intense interest in chemistry, physics, and most recently, information theory [1,2]. Over the past several years, it has become clear that the physical implementation of logical gates in quantum information processing (QIP) may be facilitated by using the methods of optimal control theory (OCT) to maximize the gate fidelity with a target quantum gate [3–7]. Such implementations have been directed toward discrete QIP, as hypothetically carried out on the so-called quantum spin computers originally discussed by Benioff and Feynman [8,9]. These computers, in which information is carried as quantum bits (qubits) [10] encoded in discrete systems like electron spins or two-level atoms, are the quantum version of digital classical computers. Analog to classical information carried by a continuous (analog) signal, quantum information can also be carried by (infinite-dimensional) continuous quantum systems, such as a harmonic oscillator, rotor, or modes of the electromagnetic field [11]. Quantum information processing over continuous variables (CV) can be thought of as the systematic creation and manipulation of continuous quantum bits, or qunits [11].

Importantly, continuous-variable quantum information processing (CVQIP) may be less susceptible to drift than its classical counterpart. Cleverly encoded quantum states can be restandardized and protected from the gradual accumulation of small errors, or from the destructive effects of decoherence [12]. Moreover, compared to its discrete counterpart, CVQIP has several practical advantages, originating, for example, in the high bandwidth of continuous degrees of freedom, that have spurred substantial interest in its generic properties. Significant experimental advances have recently been made, including the demonstration of quantum teleportation over continuous variables [13]. As experimental methodologies improve, it becomes important to consider how such implementations can be enhanced through the systematic application of OCT.

Here, we examine OCT problems pertaining to an important class of continuous quantum gates, namely those that can be represented as symplectic transformations of the quadrature vectors in the Heisenberg picture. This gate set is referred to as the Clifford group [14], which, according to the generalized Gottesman-Knill (GK) theorem, are sufficient to represent any CV quantum computation that can be efficiently simulated on a classical computer (as such, the symplectic gate formalism also has applications in the context of reversible analog classical computation). Although universal quantum computation over continuous variables requires higher-order nonlinear operational gates, networks using only Clifford group gates have numerous important applications in the area of quantum communication, and in fact, these gates are in many ways easier to implement over continuous variables than over discrete variables [15]. For example, quantum error correcting codes, which are essential for overcoming the effects of errors and decoherence, use only Clifford group gates for encoding and decoding. Other important protocols in QIP, like quantum teleportation, also rely solely on Clifford group gates and related measurements.

Early control studies on continuous quantum systems focused on the manipulation of quantum scattering states in bond-selective control (i.e., dissociation or association) of molecular systems [16,17], where OCT can be effectively applied. In this paper, we investigate the implementation of CV quantum gates via OCT, where the distance between the real and ideal quantum unitary transformation is used as a metric for assessing optimality. Prior work [18] has begun to examine the question of constructing minimal time quantum circuits for a given symplectic gate from restricted control Hamiltonians. Here, we are concerned with the general problem of implementing symplectic gates in arbitrary time with unrestricted quadratic control Hamiltonians. By contrast, we are interested in the general problem of gate control for arbitrary quadratic Hamiltonians and arbitrary final times.

We carry out this analysis in two stages. First, we analyze the features of the optimal control landscape for symplectic gate fidelity, defined as the map between admissible controls and associated values of objective function. Such landscapes were recently shown to universally possess very simple critical topologies for finite-dimensional quantum gates, with no suboptimal traps impeding optimal searches, irrespective of the system Hamiltonian for controllable systems [19]. Upon the assumption of full controllability of the underlying control systems, the control landscapes for symplectic gates are also free of local traps that might otherwise impede the optimization process. Next, we carry out numerical OCT calculations for various CV gates, comparing to the analogous discrete variable gates with two physical models. We identify characteristic differences between these two problems in terms of control optimization efficiency, the factors influencing maximum achievable gate fidelity, and the physical properties of the associated optimal Hamiltonians.

The paper is organized as follows. Section II provides preliminaries on the symplectic gates applied in CVQIP and discusses several representative models for their physical implementation. Section III examines analytical features of the optimal control landscape for CV gate control and describes numerical algorithms for searching this landscape. In Sec. IV, we carry out OCT calculations for specific CV gates and algorithms using these representative model Hamiltonians, comparing with the corresponding problems for discrete quantum gates. Finally, Sec. V draws general conclusions regarding OCT for CV quantum gates versus discrete quantum gates.

II. SYMPLECTIC GATES AND CONTROL SYSTEM MODELS

The optimal control theory for CV gates frames the time evolution of the canonical observable operators over the symplectic group [20]. As such, these gates are represented by symplectic propagators. This section will provide necessary preliminaries on symplectic gates and their realization via dynamical controls.

A. Symplectic gates

For simplicity, suppose that the CV system is to be realized as a quantized electromagnetic field. Let $\hat{a}_j$ and $\hat{a}_j^\dagger$ represent the creation and annihilation operators corresponding to the jth mode of the field. These operators are related to the position and momentum operators by

$$\hat{q}_j = \frac{1}{\sqrt{2}}(\hat{a}_j + \hat{a}_j^\dagger),$$

$$\hat{p}_j = \frac{1}{\sqrt{2}}(\hat{a}_j - \hat{a}_j^\dagger).$$

Denote $\hat{z}=(\hat{q}_1,\ldots,\hat{q}_N;\hat{p}_1,\ldots,\hat{p}_N)$ the quadrature vector and let U be a unitary transformation over it through

$$U:\hat{z}_\alpha \mapsto U^\dagger \hat{z}_\alpha U = \sum_\beta S_{\alpha\beta}\hat{z}_\beta,$$

where the matrix S is an element of the symplectic group $\mathrm{Sp}(2N,\mathbb{R})$ defined as the set of $2N\times 2N$ matrices such that $S^TJS=J$, where

$$J = \begin{pmatrix} & I_N \\ -I_N & \end{pmatrix}.$$

Here the matrix S captures the Heisenberg equations of motion for the operators $\hat{z}_i$, and the unitary propagator U forms the metaplectic unitary representation of S in $\mathrm{Sp}(2N,\mathbb{R})$. Another important class of transformations over the CVs are the displacements that shift $\hat{q}$ and $\hat{p}$ by constants:

$$\hat{q} \mapsto \hat{q} + a,$$

$$\hat{p} \mapsto \hat{p} + b. \tag{1}$$

The combination of displacements with homogeneous symplectic transformations forms the Clifford group, or the inhomogeneous symplectic group $\mathrm{ISp}(2N,\mathbb{R})$, in the form of

$$S_c = \begin{pmatrix} S & c \\ 0 & 1 \end{pmatrix}, \quad S \in \mathrm{Sp}(2N,\mathbb{R}), \quad c \in \mathbb{R}^{2N},$$

which acts on the extended quadrature vector $H_2=a^\dagger b_2^\dagger + ab_2$.

In the context of quantum optics, which is the basis of most proposed schemes for CV quantum computation, the symplectic gates require both linear and nonlinear optics. The linear elements (such as beam splitters, mirrors, and half-wave plates) include the inhomogeneous displacement transformation and the maximal compact subgroup $\mathrm{OSp}(2N,\mathbb{R})$ of orthogonal symplectic matrices that preserve the total photon number $\hat{n}=\sum_{i=1}^N \hat{a}_i^\dagger \hat{a}_i$. The nonlinear elements (such as squeezers, parametric amplifiers, and downconverters) fall into the noncompact portion of $\mathrm{Sp}(2N,\mathbb{R})$, and correspond to photon nonconserving transformations.

There exists a set of universal symplectic gates whose combinations may realize arbitrary Clifford gates in $\mathrm{ISp}(2N,\mathbb{R})$. A well-known choice of the universal gate set consists of the (linear) Pauli operators, the Fourier gate, phase gate, and the SUM gate as described below.

(1) The Pauli operators perform the phase displacements

$$X(q_j) = \exp(i\hbar q_j \hat{p}_j),$$

$$Z(p_j) = \exp(i\hbar p_j \hat{q}_j),$$

whose symplectic representations are

$$X(q) = \begin{pmatrix} 1 & 0 & q \\ 0 & 1 & 0 \\ 0 & 0 & 1 \end{pmatrix},$$

$$Z(p) = \begin{pmatrix} 1 & 0 & 0 \\ 0 & 1 & -p \\ 0 & 0 & 1 \end{pmatrix}. \tag{2}$$

(2) The one-qunit Fourier transform is the CV analog of the discrete Hadamard gate:

$$F = \exp\left\{\frac{i}{\hbar}\frac{\pi}{4}(\hat{q}^2 + \hat{p}^2)\right\}:\begin{pmatrix}\hat{q}\\ \hat{p}\end{pmatrix} \mapsto \begin{pmatrix}\hat{p}\\ -\hat{q}\end{pmatrix}.$$

This action can be represented by a 2×2 symplectic matrix

$$F = \begin{pmatrix}0 & 1\\ -1 & 0\end{pmatrix} \in \mathrm{OSp}(2,\mathbb{R}). \tag{3}$$

(3) The phase gate is the analog of the discrete variable phase gate

$$P(\eta) = \exp\left(\frac{i}{2\hbar}\eta\hat{q}^2\right):\begin{pmatrix}\hat{q}\\ \hat{p}\end{pmatrix} \mapsto \begin{pmatrix}\hat{q}\\ \hat{p}-\eta\hat{q}\end{pmatrix}.$$

Unlike the other gates, P is a function of a real parameter and can be represented by the matrix (in homogeneous form)

$$P(\eta) = \begin{pmatrix}1 & 0\\ -\eta & 1\end{pmatrix} \in \mathrm{Sp}(2,\mathbb{R}). \tag{4}$$

(4) The SUM gate acts on a two-qunit system where qunit 1 is said to be the control and qunit 2 is said to be the target [14,21], and it carries out the following transformations on the canonical observable operators:

$$\mathrm{SUM}: \quad \hat{q}_1 \mapsto \hat{q}_1, \quad \hat{q}_2 \mapsto \hat{q}_1 + \hat{q}_2, \quad \hat{p}_1 \mapsto \hat{p}_1 - p_2, \quad \hat{p}_2 \mapsto \hat{p}_2.$$

This is the continuous-variable analog of the discrete controlled-NOT (CNOT) gate and its unitary representation is

$$\mathrm{SUM} = \exp\left(-\frac{i}{\hbar}\hat{q}_1\hat{p}_2\right).$$

Therefore the associated symplectic representation in homogeneous form is

$$\mathrm{SUM} = \begin{pmatrix}1 & 0 & 0 & 0\\ 1 & 1 & 0 & 0\\ 0 & 0 & 1 & -1\\ 0 & 0 & 0 & 1\end{pmatrix} \in \mathrm{Sp}(4,\mathbb{R}). \tag{5}$$

B. Control systems for CVQIP

In this paper, we are only concerned with the optimal control of the homogeneous symplectic transformation (the inhomogeneous displacement transformations can be performed relatively easily and independently [22,23]). The system Hamiltonian $\hat{H}(t)$ required to generate such transformations are quadratic in $\hat{z}=(\hat{q}_1,\ldots,\hat{q}_N;\hat{p}_1,\ldots,\hat{p}_N)^T$, the vector of quadratures of quantum observables. The unitary propagator is manipulated through the controlled Schrödinger equation

$$\frac{dU(t)}{dt} = -\frac{i}{\hbar}[\hat{H}_0 + \sum_{i=1}^{m} C_i(t)\hat{H}_i]U(t), \tag{6}$$

where $\hat{H}_0$ is the (quadratic) internal Hamiltonian and $\hat{H}_i$ is the interaction Hamiltonian steered by a control field $C_i(t)$ to couple the internal degrees of freedoms. Suppose that $\hat{H}_i = \Sigma_{\alpha,\beta} h_{i,\alpha\beta}\hat{z}_\alpha\hat{z}_\beta$, $i=0,1,\ldots,m$, and let $H_i=\{h_{i,\alpha\beta}\}$. Through this representation, the symplectic matrix $S(t)$ associated with $U(t)$ follows a classical Hamiltonian evolution equation

$$\frac{dS(t)}{dt} = J[H_0 + \sum_{i=1}^{m} C_i(t)H_i]S(t). \tag{7}$$

Early proposals for CVQIP focused on coupled pairs of conjugate continuous variables describing quadrature modes of the electromagnetic field [11,21,24], where it is typically possible to apply only one control at any given time. More recently, CV models displaying greater flexibility have been proposed that may be more suitable for optimal control of quantum gates. In particular, these control systems allow for the simultaneous application of two or more independent controls. A simple model raised in [24,25] considered the off-resonant interaction of light with a collective spin described by the effective Hamiltonian

$$\hat{H}_0 = \kappa\hat{q}_1\hat{p}_2,$$

which represents a strongly coherent light beam polarized along the x axis that propagates along the z axis through the atomic ensemble. In addition, it is assumed that arbitrarily fast local phase shifts are implementable by single-model control Hamiltonians:

$$\hat{H}_1 = \hat{q}_1^2 + \hat{p}_1^2, \quad \hat{H}_2 = \hat{q}_2^2 + \hat{p}_2^2.$$

The control pulses are usually instantaneous and exerted in certain sequences to simplify the analysis and the experimental realization. However, here we will assume that the control pulses can be arbitrarily shaped, so that a greater degree of precision is possible in tailoring the control Hamiltonian to match theoretical predictions.

Recently, atomic ensembles, particularly ensembles of trapped ions, have emerged as a promising medium for CVQIP [26–28] because the trapped ions are thermally isolated from their environment, minimizing decoherence effects. Quantum information is stored in the vibrational modes of the trapped ions. Some quantized fields inside an optical cavity [26,27] are applied to couple (entangle) these vibrational modes, through which it is possible to indirectly tune the coupling between vibrational modes. For concreteness, consider a model wherein two trapped ions with internal electronic levels are coupled to external lasers. They are also coupled to a cavity mode with frequency ω_c, described by annihilation and creation operators $\hat{a}$ and $\hat{a}^\dagger$, respectively, where the harmonic frequency of each trap is 2ν. Assume that the cavity is oriented along the x axis and the laser is incident along the y or z axis. Then in a frame that is rotating with frequency ω_c, the interaction Hamiltonian coupling the vibrational modes of the ions with the cavity and laser fields can be written as (omitting the electronic states);

$$\hat{H} = 2\nu(\hat{b}_1^\dagger\hat{b}_1 + \hat{b}_2^\dagger\hat{b}_2) + \hat{V},$$

where $\hat{b}_{1,2}$ and $\hat{b}_{1,2}^\dagger$ are the annihilation and creation operators of the vibrational modes. The interaction Hamiltonian $\hat{V}$

is a function of the coupling constants between ions and lasers and single-photon coupling strengths. Under reasonable assumptions regarding the size of the traps compared to the laser wavelength, and with proper detuning of the lasers from the cavity mode, the interaction Hamiltonian for the first ion can be approximated as [27]

$$\hat{V} \approx r_{11}(\hat{a}^\dagger \hat{b}_1 + \hat{a}\hat{b}_1^\dagger) + r_{21}(\hat{a}^\dagger \hat{b}_2^\dagger + \hat{a}\hat{b}_2),$$

where r_{11} and r_{21} are functions of the frequencies and coupling constants. This system actually involves three harmonic oscillators, where ion-cavity interaction Hamiltonians produce indirect couplings between the vibrational modes of the two ions. By modulating the frequencies of these lasers through time, we can achieve time-dependent control Hamiltonians necessary for the implementation of CV gates with optimal fidelity. The controls in this model induce nonlocal interactions between qunits.

The above models display features that are representative of current proposals for CVQIP. The light-collective spin interaction control system (hereafter referred to as the "photon model") is a promising candidate for achieving most symplectic transformations experimentally.

C. Controllability of CV gates

Systems employed to process quantum information are generally required to be sufficiently controllable, i.e., able to realize arbitrary desired quantum gates. A fundamental necessary condition for controllability of systems evolving on general Lie groups [29] is the rank condition, i.e., the condition that the Lie algebra spanned by $H_0, H_1, \ldots, H_m$, and their commutators such as $[H_0, H_i]$, $[H_0,[H_0,H_i]]$, $[H_i,[H_0,H_j]]$, and so on, equals the Lie algebra of the Lie group. This condition has been proven to be sufficient for the unitary propagators of discrete-state quantum systems [29], and such systems are exact-time controllable for any time $t > T_0$ where T_0 is some constant positive time, i.e., arbitrary gate can be achieved exactly at any positive $t > T_0$. However, for systems on noncompact symplectic groups, the rank condition is generally insufficient except when H_0 is compact, and there is no guarantee of exact-time controllability, i.e., it may take an extremely long time for some particular gates. The controllability usually fails when H_0 is noncompact [29,30], but proper use of multiple control fields may greatly enhance it, such that any gate can be achieved at arbitrary positive times (rendering the system strongly controllable), if their corresponding control Hamiltonians span the Lie algebra of the symplectic group.

In choosing CV control systems for the purposes of our study, we are guided by two considerations: (1) the differing controllabilities of systems proposed thus far in the literature and (2) the nature of the coupling between qunits in such control schemes. Thus far, the design of CV gate control systems has not paid enough attention to the effects of the controllability of these systems on the maximal achievable gate fidelity. A reason for this oversight may be the fact that in discrete gate control, exact-time controllability is usually easy for achieving high fidelity control. With respect to the coupling between qunits, we will show that whether the controls act locally (between pairs of qubits) or nonlocally (among multiple qubits) has a dramatic impact on the efficiency of control optimization, as well as the energetic expense of implementing the optimal controls.

Assessment of the controllability of the proposed physical models described above reveals that (1) the photon model satisfies the rank condition, but is not ensured to be fully controllable because H_0 is noncompact; and (2) the ion-trap model does not satisfy the controllability rank condition, and hence is only controllable over a Lie subgroup of $\mathrm{Sp}(6,\mathbb{R})$. This lack of strong controllability is characteristic of many proposed physical models for CVQIP. Nonetheless, such schemes are still feasible for many practical gates.

In addition to the above two physical models, we also study a strongly controllable system below in order to explore the effects of controllability on the properties of gate optimization. The following control Hamiltonians were employed for this purpose:

$$\hat{H}_1 = \hat{a}_1^{\dagger 2} - \hat{a}_1^2 + \hat{a}_2^{\dagger 2} - \hat{a}_2^2,$$

$$\hat{H}_2 = \hat{a}_1^\dagger \hat{a}_1 - \hat{a}_2^\dagger \hat{a}_2 + i(\hat{a}_1^\dagger + \hat{a}_1)(\hat{a}_2^\dagger - \hat{a}_2);$$

the internal Hamiltonian in this case consisted of uncoupled harmonic oscillators, i.e., $\hat{H}_0 = \hat{a}_1^\dagger \hat{a}_1 + \hat{a}_2^\dagger \hat{a}_2 + 1$.

In the following, we make several comparisons to discrete QIP. For this purpose, we assume the standard physical model of NMR-based quantum computation [6]. In this model, the internal Hamiltonian H_0 consists of nuclear spins that are coupled in the absence of the control field. The coupling between N spins (only up to 2-qubit interactions are considered) is achieved through standard NMR coupling Hamiltonians of the form:

$$H = \sum_{i=1}^{N} \omega_i \sigma_i^z + \sum_{i,j=1}^{N} \sum_{\alpha,\beta=x,y,z} J_{ij}^{\alpha,\beta} \sigma_i^\alpha \otimes \sigma_j^\beta + \sum_{i=1}^{N} C_i(t) \sigma_i^x,$$

where $\sigma_i^{x,y,z}$ are the standard Pauli matrices representing observables of the ith qubit. The first term splits the energy levels via a static magnetic field along the z axis, with ω_i being the Raman frequencies; the second term represents the internal couplings between the qubits (e.g., chemical shifts); the last term, the control Hamiltonian, interacts each qubit state to a time-variant x-axis radio-frequency control field $C_i(t)$. Because of the tensor product structure of qubit subspaces in these expressions, the total system dimension scales as 2^N. One can verify that this system is controllable, but not strongly controllable.

III. OPTIMAL CONTROL OF SYMPLECTIC GATES

The objective of this paper is to identify the time-dependent functional form of the Hamiltonian that minimizes the distance to a target symplectic (CV) gate at a fixed time t_f, with a particular focus on the convergence of search algorithms for this problem. Since the (quantum) symplectic gate $U(t)$ is a faithful unitary representation of a symplectic matrix $S(t)$, it is reasonable and convenient to define the gate fidelity analogously to that for discrete gates as

$$\mathcal{F}[C(\cdot),t_f] = \mathrm{Tr}[S(t_f) - W]^T[S(t_f) - W], \tag{8}$$

where W is the finite-dimensional representation of the target quantum propagator, and $S(t_f)$ is the representation of the system propagator $U(t_f)$ as an implicit function of $C(\cdot)$. In this section, we describe numerical algorithms used to search for optimal controls and study analytical features of the symplectic gate control problem via landscape analysis.

A. Numerical implementation

Several optimization algorithms, including iterative methods such as the Krotov algorithm [3] and tracking methods such as D-MORPH (diffeomorphic modulation under observable preserving homotopy) [31], have been applied in the OCT of discrete quantum gate implementations. These algorithms can vary considerably in optimization efficiency, but they are all based on information pertaining to the first functional derivative of the objective function with respect to the control field. Here we adopt gradient algorithms to search for optimal controls, which, although not the most efficient, offer the simplest and most direct opportunity for comparing the properties of discrete and continuous gate OCT. In particular, they are ideal for detecting landscape traps.

The electric field $C_i(s,t)$ was restricted to be piecewise constant over $[0,t_f]$, i.e., they are constant on each equally divided subintervals $[t_k,t_{k+1}]$ $k=1,\ldots,q$, with $t_1=0$ and $t_k=t_f$. The field is stored as a q-dimensional vector in each algorithmic step s_j. Starting from an initial guess $C_i(s_0,\{t_k\})$ for the control field, the equations of the motion were integrated over the interval $[0,t_f]$ by propagating the Schrödinger equation over each time step $t_k \to t_{k+1}$, producing the local propagator $U(t_{k+1},t_k)=\exp[-iH(s_j,t_k)t_f/q]$, while for symplectic case the local propagator is $S(t_{k+1},t_k)=\exp[JH(s_j,t_k)t_f/q]$.

The Pade approximation for the exponential function was used to calculate the local symplectic propagators $S(t_{j+1},t_j)=\exp[JH(s_i,t_j)t_f/(q-1)]$. Since the matrix $JH(s_i,t_j)$ is not symmetric, it is not possible to calculate its exponential via diagonalization and subsequent scalar exponentiation of its eigenvalues. The type (p,q) Pade approximation for e^x is the (p,q)-degree rational function $P_{pq}(x)\equiv N_{pq}(x)/D_{pq}(x)$ obtained by solving the algebraic equation $\sum_{k=0}^{\infty}x^k/k! - N_{pq}(x)/D_{pq}(x)=O(x^{p+q+1})$, i.e., $P_{pq}(x)$ must match the Taylor series expansion up to order $p+q$. Due to the large number of iterations generally required for convergence of CV quantum controls, the speed of the matrix exponentiation algorithm is particularly important. In contrast to discrete gates, acceleration of matrix exponentiation for CV systems via the propagation toolkit requires significantly greater memory overhead for the storage of precomputed propagators at discrete control field intervals. Otherwise, discretization of the control field amplitudes produces unacceptable errors in the matrix exponential, and the maximum amplitudes often grow abruptly during optimization. However, for larger systems where the number of iterations for convergence increases considerably, the storage overhead will be warranted due to the resulting substantial increase in propagation speed per step.

Theoretically, the gradients of the objective functions can be proven to be

$$\frac{\delta\mathcal{F}(S)}{\delta C_j(t)} = \mathrm{Tr}\{H_j(t)J[S^T(t_f)W - W^TS(t_f)]\},$$

where $H_j(t)=S^T(t)H_jS(t)$, for CV gates, and

$$\frac{\delta\mathcal{F}(U)}{\delta C_j(t)} = i\ \mathrm{Tr}\{H_j(t)[U^\dagger(t_f)W - W^\dagger U(t_f)]\},$$

where $H_j(t)=U^\dagger(t)H_jU(t)$ for discrete unitary gates. Here, the H_j is the Hamiltonian that couples to the time-dependent control $C_j(t)$. Since the field is constrained to be piecewise constant, the system at each time instance t_k can be precisely represented as the product of these local propagators:

$$U_k = U(t_k,t_{k-1})\cdots U(t_2,t_1),$$

$$S_k = S(t_k,t_{k-1})\cdots S(t_2,t_1),$$

where $U_1=I_N$ and $S_1=I_{2N}$. For the application of numerical gradient algorithms, the gradient vector is discretized as follows:

$$\frac{\delta\mathcal{F}(S_q)}{\delta C_j(t_k)} = \mathrm{Tr}[S_k^TH_jS_kJ(S_q^TW - W^TS_q)], \quad k=1,\ldots,q,$$

$$\frac{\delta\mathcal{F}(U_q)}{\delta C_j(t_k)} = i\ \mathrm{Tr}[U_k^\dagger H_jU_k(U_q^\dagger W - W^\dagger U_q)], \quad k=1,\ldots,q.$$

Among gradient algorithms [32], the conjugate gradient (CG) method applied here is among the most efficient existing implementations. Here we minimize the fidelity function using the Polak-Ribere variant of the CG method with step size varied adaptively based on Brent's method for line minimizations. In several cases, an adaptive step size steepest descent algorithm was employed to analyze the behavior of gradient flow lines.

Optimization algorithms for CV gate control are inherently more susceptible to instabilities than those for discrete gate control due to the appearance of positive real eigenvalues in the exponent of the dynamical propagator matrix exponential, which makes it easy to propagate the symplectic operators toward infinity. In the case of the gradient, however, the following topology analysis indicates that the algorithm is fundamentally stable, i.e., that the search for optimal controls monotonically decrease to cost value $\mathcal{F}$ and guide the iterations to the unique global optimum. Nonetheless, in practice, finite numerical precision can in certain cases cause artificial instabilities in gradient algorithms for CV control optimization. This may occur when the initial guess for the control field results in the corresponding symplectic propagator being very far from the global optimum, or the norm of the corresponding gradient vector exploding to infinity, so that the actual iteration process deviates away from the ideal gradient flow and leads to instability. These problems can be avoided by carefully choosing the initial guess of control fields. Another commonly used class of algorithms in OCT of classical dynamical systems consists of iterative algorithms based on Pontryagin's maximum principle [33]. These are often used in conjunction with gradient algorithms to speed up optimization in the vicinity of the solution, but are much more susceptible to instabilities away from the optimum. This is another reason that gradient algorithms are adopted in this paper.

B. Landscape topology and its impact on control search

Theoretically, an optimal control solution is a critical point of the gate fidelity function $\mathcal{F}$. Since this control landscape generally has nonunique critical points, and any of them can be a candidate of the ultimate optimal solution, the topology of the critical sets is essential in estimating the complexity of searching for optimal controls [34]. Under the assumption of controllability over the symplectic group at the final time t_f, the topological analysis [35] of the critical points of the landscape (8) in the domain of admissible control fields can be reduced to that of

$$\mathcal{F}(S) = \|S - W\|^2$$

over a smaller space $\mathrm{Sp}(2N,\mathbb{R})$, because in that case each critical control is locally maximal (minimal, saddle) if and only if the resulting $S(t_f)$ is locally maximal (minimal, saddle). In [35,36], it is shown that the set of critical points consists of a finite number of critical submanifolds that can be expressed as [35]

$$S^* = UR^TDRV, \quad R \in \mathrm{stab}(E), \tag{9}$$

where the matrices U, V, and E are from the singular value decomposition of $W=UEV$. The stabilizer $\mathrm{stab}(E)$ of E in $\mathrm{OSp}(2N,\mathbb{R})$ is defined as

$$\begin{aligned}\mathrm{stab}(E) &= \{R \in \mathrm{OSp}(2N,\mathbb{R}) | R^TER = E\}\\ &= \mathrm{OSp}(2n_0) \times O(n_1) \times \cdots \times O(n_s).\end{aligned}$$

Suppose that the singular values of the diagonal matrix E are $e_s^{-1} < \cdots < e_1^{-1} = 1 = e_0 < e_1 < \cdots < e_s$, where the degeneracies for $e_1,\ldots,e_s$ are $n_1,\ldots,n_s$ as well as those of $e_1^{-1},\ldots,e_s^{-1}$. The characteristic matrix D contains different operations on the separate modes represented by its diagonal blocks (their inverses appear pairwise symmetrically in D and E according to the reciprocal property of eigenvalues of symplectic matrices) as follows [35].

(1) Type-I operations $D'_\alpha = e_\alpha I_{m'_\alpha}$ corresponding to a subblock $E'_\alpha = e_\alpha I_{m'_\alpha}$ in E, which are identical with those operations in the target transformation W.

(2) Type-II operations $D''_\beta = -e_\beta^{1/3} I_{m''_\beta}$ corresponding to a subblock $E''_\beta = e_\beta^{-1} I_{m''_\beta}$ in E, which reverse the directions of the quadrature vector of the corresponding modes and is followed by a squeezing operation with ratio $e_\beta^{1/3}$ on the $\hat{q}$ components.

(3) Type-III operations

$$D_{\gamma\delta} = \sqrt{\frac{e_\delta}{e_\gamma}} \begin{pmatrix} \cos x_{\gamma\delta} I_{m_{\gamma\delta}} & \pm \sin x_{\gamma\delta} I_{m_{\gamma\delta}} \\ \pm \sin x_{\gamma\delta} I_{m_{\gamma\delta}} & -\cos x_{\gamma\delta} I_{m_{\gamma\delta}} \end{pmatrix},$$

where $x_{\delta\gamma} = \arccos \frac{e_\gamma/e_\delta - e_\delta/e_\gamma}{(e_\delta e_\gamma)^{1/2} - (e_\delta e_\gamma)^{-1/2}}$, corresponding to a subblock

$$E_{\gamma\delta} = \begin{pmatrix} e_\gamma I_{m_{\gamma\delta}} & \\ & e_\delta^{-1} I_{m_{\gamma\delta}} \end{pmatrix}, \quad e_\delta^{1/3} \le e_\gamma \le e_\delta,$$

which rotates two decoupled γth and δth modes with an angle $x_{\delta\gamma}$ followed by a uniform squeezing operation on both modes.

(4) The subblock for the particular singular value $e_0 = 1$ is

$$D_0 = \begin{pmatrix} I_{m_0} & \\ & -I_{n_0 - m_0} \end{pmatrix},$$

which leaves m_0 modes of linear operations invariant and reverses the direction of quadrature vectors of the other $n_0 - m_0$ modes in the phase space.

It is apparent that the overall landscape topology is influenced greatly by the compactness and degeneracies of the singular values of W, which determine the number and possible structures of the critical submanifolds. In [35] we found that the landscape has only one locally minimal critical submanifold, and the remaining critical submanifolds are all saddles. This greatly facilitates the search for optimal control fields, implying that local algorithms will eventually converge to the desired optimal solutions without being trapped by any suboptima. Absence of local traps is a property also shared by the landscape for the discrete-variable quantum gate control [19], where

$$\begin{aligned}\mathcal{F}(U) &= \mathrm{Tr}(W-U)^\dagger (W-U) = 2N\\ &\quad - 2\,\mathrm{Re}\,\mathrm{Tr}(W^\dagger U), \quad U \in \mathcal{U}(N),\end{aligned} \tag{10}$$

with $W \in \mathcal{U}(N)$ representing the target unitary transformation. However, the critical topology for the landscape (10) is universal, i.e., independent of W as well as the implemented Hamiltonians, while the topology for Eq. (8) strongly depends on the target gate W.

Each combination of the indices $\{m_0, m'_\alpha, m''_\beta, m_{\gamma\delta}\}$ labels an individual critical submanifold. All admissible combinations can be enumerated to count the number of the critical submanifolds, which is always finite. The number of critical manifolds in the control landscape scales linearly as $N+1$ when W is compact (e.g., F, X, and Z or combinations thereof), where N is the number of qunits. This scaling is the same as that of a discrete quantum gate where N is the number of levels [19].

When W is noncompact but has fully degenerate singular values, this scaling can be shown to be quadratic in N [35]:

$$\mathcal{N} = \begin{cases} (N+2)^2/2, & N \text{ even;} \\ (N+1)(N+3)/2, & N \text{ odd.} \end{cases} \tag{11}$$

The scaling for nondegenerate gates keeps rising when the degeneracy is broken. For the extremal case that W has fully nondegenerate singular values, the upper bound for the number of critical submanifolds is

$$\mathcal{N}_1 = \sum_{m=1}^{[N/2]} \frac{2^{N-3m} N!}{m!\,(N-2m)!},$$

which is superexponential but lower than $N!$ scaling. Figure 1 compares the above scalings with that of (N-level) unitary

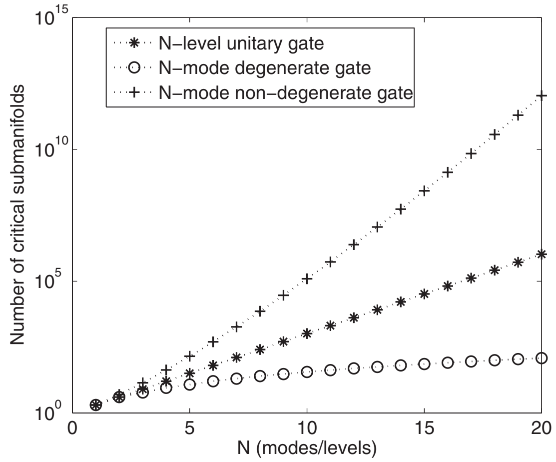

FIG. 1. The scaling of the numbers of critical submanifolds for fully nondegenerate (N-qunit) symplectic gates and (N-qubit) unitary gates.

gates, showing that the number of critical submanifolds for N-qunit symplectic gates always grows faster than that for N-level unitary gates. This implies that the search for optimal controls will be more slowed down on the symplectic group than on the unitary group.

Since all these critical submanifolds are orbits of a compact Lie group stab(E), they must be contained in the ball centered at W with radius $R\sim\sqrt{N}$ equal to the distance to the farthest critical points, wherein they may affect the optimal search. The volume of this region is roughly of the order $V\sim N^{N^2}$, which rises so quickly as N increases that it is expected that the probability for a random initial guess to be close to a saddle manifold should be small enough to be negligible in practice.

The above results apply when controls are applied using both linear optics and squeezing. We are also interested in the optimal control problem that involves the use of only linear optical operations, whose realizable CV gates S are restricted to the compact symplectic group $\mathrm{OSp}(2N,\mathbb{R})$. In [35,36], it is shown that the landscape topology for this problem is identical to that of discrete-variable gate control over $\mathcal{U}(N)$ due to the isomorphism between $\mathrm{OSp}(2N,\mathbb{R})$ and $\mathcal{U}(N)$. For a compact target symplectic gate, the critical submanifolds are completely identical when the search is carried out on the full symplectic group (corresponding to linear optics plus squeezing) or its compact subgroup (corresponding to only linear optics), the only difference being an increase in the dimension of the search space. Therefore the additional directions accessible through squeezing transformations are not expected to improve convergence toward the optimal solution. These observations collectively draw a fairly simple picture of CV gate landscape topology, which, although more complicated than the topology of discrete gate landscapes, should not preclude efficient control optimization.

Throughout this paper, we will use gradient algorithms to optimize the control field. The search process in the kinematic picture can be represented by the so-called gradient flow on the symplectic group:

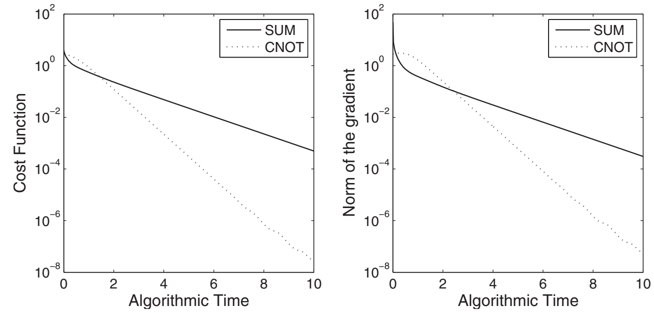

FIG. 2. The convergence of the gradient flows for optimal search of the SUM gate on $\mathrm{Sp}(4,\mathbb{R})$ and CNOT gate on $\mathcal{U}(4)$.

$$\frac{dS}{ds}=-\nabla\mathcal{F}(S),$$

where the parameter s is the algorithmic time representing the progress of iterations. It is instructive to estimate the convergence speed of the gradient flow. Via linearization of this equation in a sufficiently small neighborhood of the global optimum $S=W$, one can observe that the gradient vector converges approximately exponentally to zero (acommpaning with proper line search methods) and the converging rate is dominated by the smallest eigenvalue of the Hessian form at W, identified as $\omega_{\max}^{-2}\leq 1$, where $\omega_{\max}$ is the maximal singular value of W (see details in [35]). In the context of quantum optics, this parameter represents the maximal squeezing ratio of optical modes under this transformation. By comparison, a similar estimate for gate search on the discrete unitary group reveals a constant convergence rate of 1 (i.e., no squeezing). Therefore the search for noncompact symplectic gates will display slower convergence in general, depending on the magnitudes of the singular values of the target gate. Figure 2 shows the convergence speed of gradient flows for the SUM gate on the symplectic group, and, for comparison, the CNOT gate on the unitary group. In a physical context, the convergence speed for the phase gate (or squeezing gate) decreases with increasing phase shift (or squeezing ratio).

IV. NUMERICAL SIMULATIONS

In this section, we numerically solve for optimal control fields for implementing Clifford group gates and composite CV algorithms, and compare the optimization effort and control field complexity to those of the corresponding gates over discrete variables. As such, we aim to identify distinguishing features of CV gate control that will have the greatest impact on its computational and experimental implementation.

These results indicate that conjugate gradient algorithms are successful at locating optimal controls for each of the important classes of CV gates, and for each of the representative CV control systems described above. From the point of view of physical implementation of these control systems, we examine the effects of three characteristic features of CV gate control on the properties of the optimal fields. These are (A) the controllability of the CV gate control system (i.e., whether it is strongly controllable, weakly controllable, or

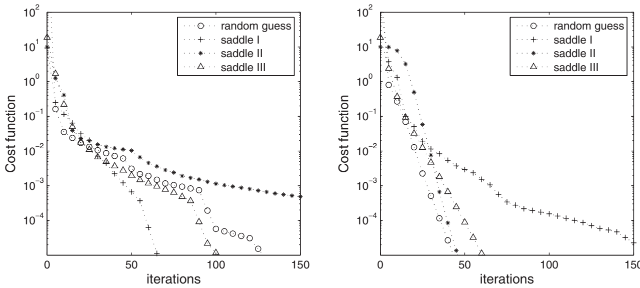

FIG. 3. The convergence of dynamical search for the SUM gate using conjugate gradient algorithms with the photon model (left) and a strongly controllable system (right).

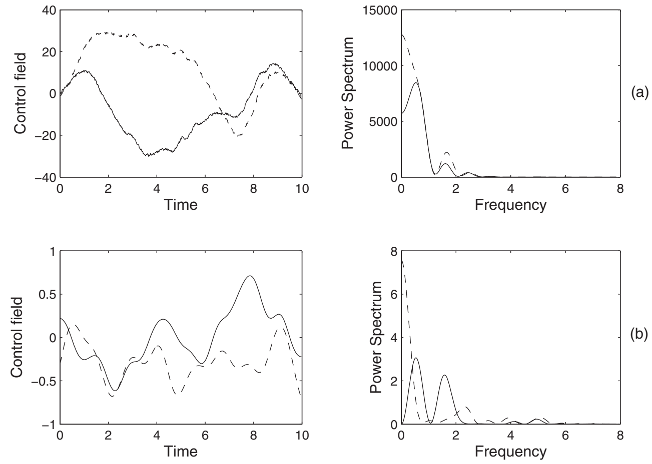

FIG. 4. The optimal control fields for CV SUM gate control after searching from a random initial guess, for (a) the photon model and (b) a strongly controllable model.

uncontrollable); (B) the compactness or noncompactness of the gate in question; and (C) the nature of the couplings between qunits. As we will show below, these features have surprisingly important effects on the feasibility of implementing proposed information processing schemes, features that have hitherto been largely ignored in the literature. By proper choice of the control system, the optimization domain, and the couplings between qunits, it is possible to engineer physical systems for CV quantum information processing in which it will be easiest to implement gates with optimal fidelity.

A. Effects of exact-time controllability on CV gate fidelity

In order to assess the effects of exact-time controllability on control fidelity, optimization efficiency, and the energy expenditure required for control, we studied the control problem where W is the SUM operation whose matrix form is shown in Eq. (5), using both the photon model ($\kappa=1$) and the strongly controllable system described above. Figure 3 compares the effects of strong versus weak controllability on convergence speed, starting from either a random guess or near saddle solutions. Although the SUM gate is reachable with both models at the final time, the weaker controllability of the photon model compromises convergence speed. In addition, Fig. 4 shows that the corresponding optimal control fields are more expensive in that their fluences are much greater.

Both the photon model and the strongly controllable model have the same kinematic critical topology, which includes a total of five critical submanifolds, including four isolated points and one one-dimensional manifold. Their characteristic indices are summarized in Table I. As discussed above, the saddles are expected to be rarely encountered during the progress of most optimization trajectories. This is supported by the simulation result (Fig. 3); the saddle manifolds appear to have a slightly adverse effect on optimization efficiency for the strongly controllable system, and have almost no influence on the convergence of the photon model.

Note that the free Hamiltonian for the photon model happens to be proportional to the matrix logarithm of the SUM gate; thus using this model, SUM can be achieved merely via free evolution in κ^{-1} units of time. Simulations show that the SUM gate is always realizable in any time longer than κ^{-1} (e.g., Fig. 4). The attempts to employ a final time less than κ^{-1} failed as shown in Fig. 5, where the control search does not converge, implying the κ^{-1} should be the minimum time required for the SUM gate. By contrast, for the strongly controllable system, optimal control fields exist even for very small t_f, although the expense increases and the shape of control fields tends to become more singular (Fig. 6).

An important feature not shown in the figures is that the optimal search can suffer from numerical instabilities when it starts far away from W (for example, when there is no *a priori* knowledge of an appropriate choice for the control fields) because the system dynamics involves exponentially increasing components. Our simulations show that this problem can be solved by sampling multiple initial control fields to get the search started close enough to the ball containing the critical points, and using sufficiently small step sizes to avoid large numerical errors. In fact, gradient algorithms are less susceptible to such numerical instabilities than faster iterative optimization algorithms, which has led to the com-

TABLE I. Critical topology for the SUM gate, where D_0 is the manifold dimension and $D_\pm$ are the numbers of positive and negative Hessian eigenvalues that reflect the optimality status.

Number	Critical value	D_0	D_+	D_-	Type
1	0	0	14	0	Minimum
2	18.623	0	10	4	Saddle
3	9.311	1	12	1	Saddle
4($\pm$)	10	0	11	3	Saddle

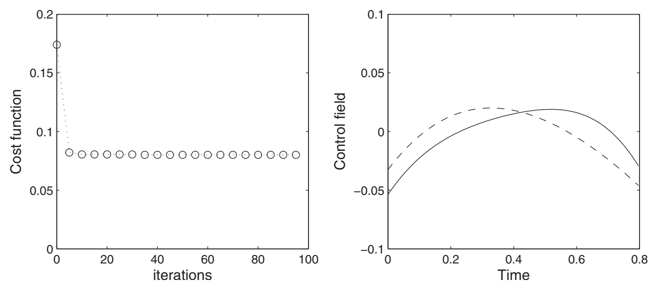

FIG. 5. Optimal control search for the SUM gate using conjugate gradient algorithms with the photon model at a final time smaller than κ^{-1}.

mon strategy in classical OCT optimization of employing gradient algorithms in the initial stages of control field search, followed by the use of iterative techniques only within a small radius of the solution [33]. By contrast, because of the compactness of the dynamical group, the control optimization for discrete quantum systems generally does not encounter numerical instabilities.

B. Effects of linear vs nonlinear implementations on optimal controls

Since the SUM gate is noncompact, the search for its optimal controls must be carried out using both linear quantum optics and squeezing. In the case of compact gates, the important question arises as to whether the use of squeezing transformations facilitates the search for optimal controls, or whether employing only linear quantum optics is preferable.

This section simulates the optimal search of a (compact) transform that swaps the states of two qunits as follows:

$$W = \begin{pmatrix} 0 & 1 & 0 & 0 \\ 1 & 0 & 0 & 0 \\ 0 & 0 & 0 & 1 \\ 0 & 0 & 1 & 0 \end{pmatrix}.$$

For this gate, we employ the photon model with two local phase controls, using two different free Hamiltonians: (i) $H_0 = x_1 p_2$, which involves squeezing operations, and (ii) $H_0 = x_1 p_2 - x_2 p_1$, which involves only linear optics. It can be verified that these systems are controllable over (i) $\mathrm{Sp}(4,\mathbb{R})$ and (ii) $\mathrm{OSp}(4,\mathbb{R})$, respectively. The simulation results in Fig. 7 show that the optimal search restricted on $\mathrm{OSp}(2N,\mathbb{R})$ generally exhibits fast convergence, as in the case of control of discrete unitary gates. This is not surprising because the group $\mathrm{OSp}(2N,\mathbb{R})$ is isomorphic to the unitary group $\mathcal{U}(N)$ and the corresponding dynamical control system is equivalent to a N-level discrete quantum control system. By contrast, optimal control using squeezing operators as well exhibits no advantages compared to using only linear operations; in fact, the application of squeezing operators can remarkably increase the energy of the control fields (Fig. 8).

Because $\mathrm{OSp}(2N,\mathbb{R})$ is isomorphic to $\mathcal{U}(N)$, a comparison of the gradients of the fidelity on $\mathrm{Sp}(2N,\mathbb{R})$ and $\mathrm{OSp}(2N,\mathbb{R})$ sheds light not only on the comparative efficiencies of these two optimization problems, but also the origin of the slower convergence of noncompact CV gate optimization versus that of discrete gate optimization. Figure 9 displays the norm

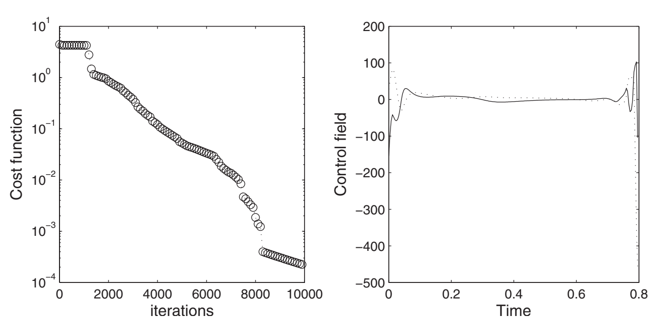

FIG. 6. Dynamical search for the SUM gate using conjugate gradient algorithms with the strongly controllable system model at a small final time.

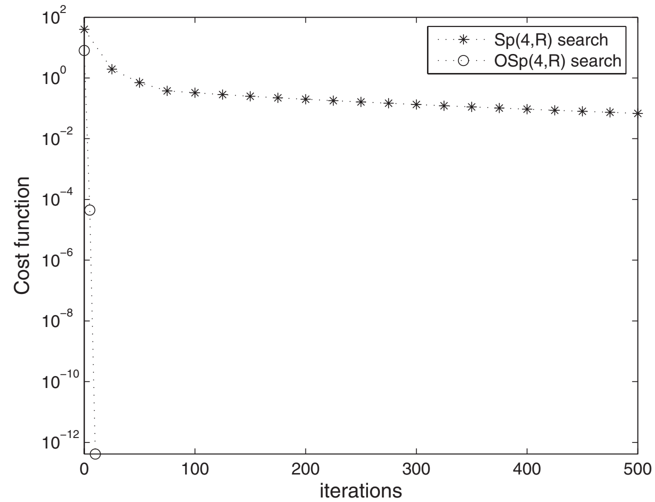

FIG. 7. The convergence of optimal search for the SWAP gate with linear and squeezing couplings $[\mathrm{Sp}(4,\mathbb{R})]$ and linear couplings $[\mathrm{OSp}(4,\mathbb{R})]$.

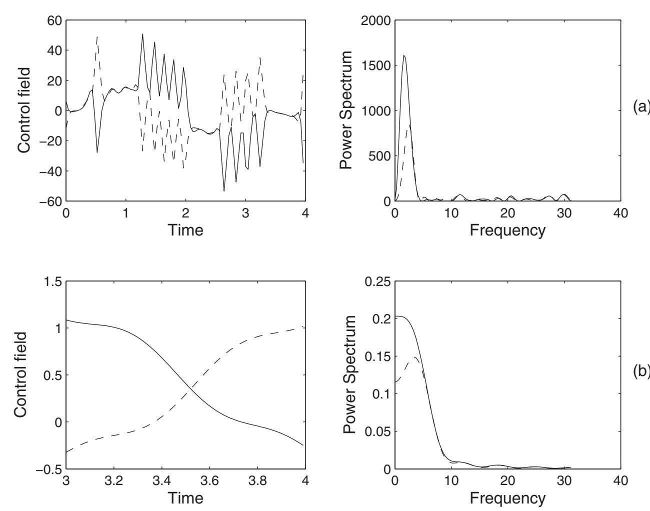

FIG. 8. The control fields for the SWAP gate with (a) linear and squeezing couplings $[\mathrm{Sp}(4,\mathbb{R})]$ and (b) linear couplings $[\mathrm{OSp}(4,\mathbb{R})]$. The solid lines refer to the control field on the first qunit, while the dotted refer to the second.

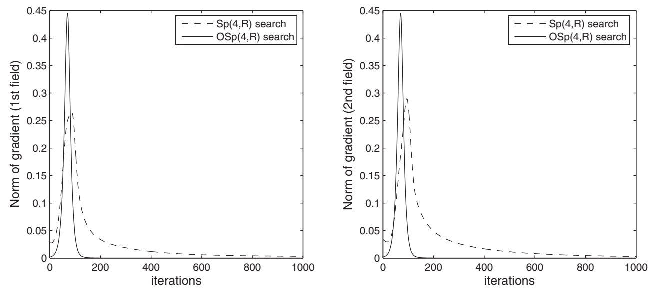

FIG. 9. The norm of the gradient vector during optimal search for the SWAP gate, starting from near a saddle point, with linear and squeezing couplings $[\mathrm{Sp}(4,R)]$ and linear couplings $[\mathrm{OSp}(4,R)]$. The left panel is for the first control field and the right panel is for the second.

of the gradient of the fidelity of the SWAP gate with respect to the control field on $\mathrm{Sp}(2N,\mathbb{R})$ and $\mathrm{OSp}(2N,\mathbb{R})$, at each algorithmic step during the course of optimization. In order to sample more points along the optimization trajectory, a steepest descent algorithm was employed in this case, starting from near a saddle point of the control landscape. As can be seen, the norm of the gradient is larger on $\mathrm{OSp}(2N,\mathbb{R})$ at most points along the optimization trajectory. In addition, over several runs, it was found that the gradient norm changes more abruptly during optimization on $\mathrm{Sp}(2N,\mathbb{R})$ compared to $\mathrm{OSp}(2N,\mathbb{R})$ [or, equivalently, $\mathcal{U}(N)$].

C. Effects of qunit-qunit coupling on optimal control energy cost

The nature of the controlled couplings between the qunits comprising multiqunit CV algorithms has a significant impact on the total energy cost of optimal control. In particular, control schemes involving only 1-qunit couplings (local controls), while physically easier to design, offer less flexibility in achieving composite multiple-qunit operations and may be temporally or energetically more costly. In order to explore this issue, we examined the optimal control of composite CV algorithms using both local and nonlocal control strategies.

Composite algorithms composed of large numbers of low-dimensional Clifford group gates will generally have richer structures in their singular values and a greater number of critical manifolds. The geometry of the control landscape is also expected to be complexified for such gates. In practice, representing composite Clifford group algorithms through sequences of 1-qunit or 2-qunit gates is generally preferred. However, since using a larger number of gates may increase the likelihood of information loss through quantum decoherence, the implementation of higher dimensional transformations is desirable in some instances.

Consider a composite operation on 3 qunits that sums the values of their q components. This gate can be decomposed into two elementary gates $\mathrm{SUM}(1,2,3)=\mathrm{SUM}(2,3)\times\mathrm{SUM}(1,2)$, which is represented by

$$\mathrm{SUM}(1,2,3)=\begin{pmatrix}1&0&0&0&0&0\\0&1&0&0&0&0\\0&1&1&0&0&0\\0&0&0&1&0&0\\0&0&0&0&1&-1\\0&0&0&0&0&1\end{pmatrix}\begin{pmatrix}1&0&0&0&0&0\\1&1&0&0&0&0\\0&0&1&0&0&0\\0&0&0&1&-1&0\\0&0&0&0&1&0\\0&0&0&0&0&1\end{pmatrix}=\begin{pmatrix}1&0&0&0&0&0\\1&1&0&0&0&0\\1&1&1&0&0&0\\0&0&0&1&-1&0\\0&0&0&0&1&-1\\0&0&0&0&0&1\end{pmatrix}.$$

This composite operation can be implemented using a photon model where the internal Hamiltonian includes interactions between 1–2 and 2–3 qunits, i.e., $H_0=x_1p_2+x_2p_3$, and three local control Hamiltonians applied in the form of $H_j=x_j^2+p_j^2$, $j=1,2,3$. Again, because the internal Hamiltonian H_0 is noncompact, full controllability is not guaranteed at arbitrary final time t_f. In the case of the ion trap model, the internal Hamiltonian H_0 consists of uncoupled harmonic oscillators, and two nonlocal controls

$$H_1=a^\dagger b_1+ab_1^\dagger,$$

$$H_2=a^\dagger b_2^\dagger+ab_2$$

are applied. As discussed above, there is no guarantee that the gate will be reachable at any final time within this model, since the system does not satisfy the controllability rank condition. In Fig. 10, we compare the convergence speeds of optimal control search for the 3-qunit SUM gate using these models with that of its discrete quantum counterpart, the controlled-CNOT gate (Toffoli gate). In the latter case, the NMR control system described above was used.

From Fig. 11, we observe a stark difference in the fluence of the optimal control fields obtained using local versus nonlocal controls. For the photon model (local controls), the fluence of the optimal fields exceeds physical limits, whereas for the ion trap model (nonlocal controls) and the NMR model, the fluence remains bounded. This indicates that for composite gates, CV control models employing nonlocal controls may be preferable to those whose design requires the use of local controls. Note that although the NMR model employs local controls, their fluence remains small, suggesting that this problem does not arise for discrete variable gates.

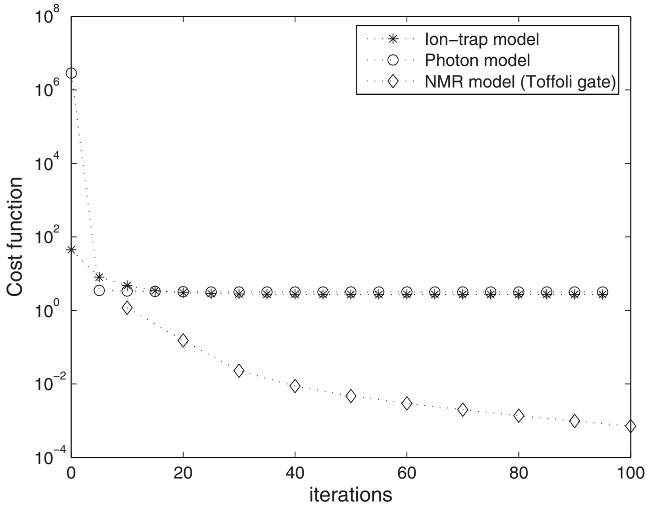

FIG. 10. The convergence of optimal searches for the 3-qunit SUM gate with photon model and ion-trap model, and 3-qubit controlled-CNOT gate with the NMR model.

This example also sheds further light on the effects of exact-time controllability on optimal control fidelity and the scaling of control search effort with system size. As can be seen from Fig. 10, neither the ion trap nor the photon control search converges within the specified tolerance for the chosen final time, whereas the strongly controllable system does converge. The weakly controllable and uncontrollable systems therefore display similar behavior for this composite gate. Thus the example demonstrates that it is even more essential to verify the controllability of a CV gate control system for higher dimensional gates.

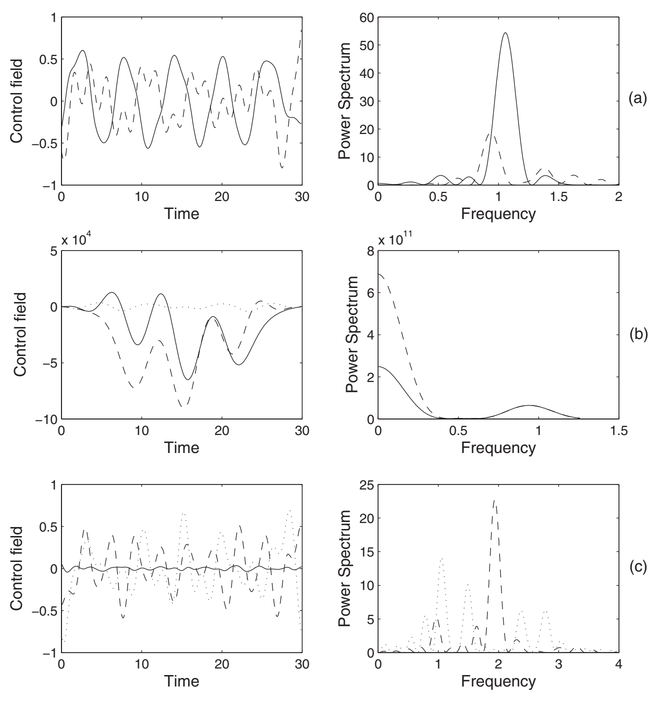

FIG. 11. The optimal control fields for (a) 3-qunit SUM gate with ion trap model, (b) 3-qunit SUM gate with photon model, and (c) 3-qubit controlled-CNOT gate. For (b) and (c), the solid (dashed, dotted) lines are the control fields on the first (second, third) qunit/qubit.

For both discrete and continuous quantum systems, the decrease in convergence speed with increasing system dimension appears to be severe; in addition, control field searches are more likely to become trapped due to easier loss of controllability. Therefore for a quantum algorithm involving a polynomially large number of operations (i.e., primitive gates), it would indeed appear more efficient to apply sequences of smaller gates rather than attempting global search over transformations on the whole set of qunits.

V. DISCUSSION

The absence of local traps in control landscapes for symplectic gate fidelity indicates that given sufficient time, local gradient-based algorithms will generally succeed at reaching the global optima (perfect fidelity), assuming the system is controllable. This property, combined with other attractive features of continuous QIP such as the high bandwidth of continuous degrees of freedom, strengthens the feasibility of QIP over continuous variables. We have demonstrated numerically across all major classes of primitive CV quantum gates, and across several canonical physical models for CV information processing, that conjugate gradient algorithms are generally capable of locating controls attaining the maximal achievable gate fidelity.

Because the dynamical propagator for CV quantum systems can have exponentially increasing components, the stability of OCT algorithms is of paramount importance. In particular, perhaps the most common type of OCT algorithm for discrete systems—iterative algorithms—is known to encounter instabilities in classical OCT problems, where the system dynamics are also governed by symplectic propagators. In these cases, it is common to employ gradient algorithms in order to control instabilities, as we have done here. In the present case, analytical evidence was provided that such algorithms should converge exceptionally well to the global optimum for sufficiently small step sizes.

We have seen that CV gate optimization problems can be divided into two classes with inherently different difficulties. The first, wherein only linear Hamiltonians are employed as controls, is mathematically identical to the problem of discrete unitary gate optimization. The second, in which squeezing operations are also employed, is generally more expensive.

A second point of distinction between these two control problems is the complexity of the optimal fields. The optimal fields for discrete gate control are typically in resonance with the transition frequencies of the system, within the weak-field regime. By contrast, in the case of CV gate optimization over $\mathrm{Sp}(2N,\mathbb{R})$, the fields are usually not simply related to any natural resonant frequencies because of the appearance of real Hamiltonian eigenvalues in the argument of the matrix exponential governing the dynamical propagation. These eigenvalues produce exponentially increasing and decreasing modes in the field. The former can result in instabilities during the optimization process [38]. Moreover, for CV gate optimization over $\mathrm{Sp}(2N,\mathbb{R})$, there is a strong dependence of field complexity on the final dynamical time. It is important to identify several controllable t_f's and choose the one corresponding to control fields that are physically the most simple to implement. However, the higher degeneracy of these fields means that we are presented with more choices for convenient physical implementation and points to a rich variety of distinct control mechanisms that reach the same objective.

The fundamentally different requirements for exact-time controllability of dynamical systems evolving on compact versus noncompact Lie groups has a dramatic effect on the maximal achievable fidelity of CV quantum gates. These effects of controllability have largely been ignored in the design of putative systems for CV quantum information processing. The present results indicate that better physical CV control systems may be designed through the application of the rank condition and numerical analysis. In particular, exact-time controllability usually fails when H_0 is noncompact [29,30]. In such cases, it is often difficult to identify a final dynamical time t_f at which the gate can be reached with high fidelity. Moreover, several current physical models for CV gate synthesis are not fully controllable for any choice of t_f. For these systems, even when the gate of interest is reachable, the cost of optimal search is typically steep. The use of multiple control fields can restore exact-time controllability if their corresponding control Hamiltonians span the whole Lie algebra of the symplectic group. While this condition is not satisfied for many proposed control systems, it can easily be introduced into future proposals.

Application of OCT to practical CV quantum information tasks will require the imposition of penalty terms on the control Hamiltonians corresponding to physical constraints. We have shown how the total energy cost of control can be delimited by carefully tuning the coupling between qunits in information processing models. Another practical limitation is the ability to shape controls to match theoretical predictions. For control of discrete states in molecular systems, current pulse shaping technologies are capable of producing the majority of shapes predicted by OCT. Ongoing efforts to design pulse shapers with ultrahigh bandwidth should further facilitate implementation of the theoretically predicted fields. For CV systems, it is difficult to shape control pulses within certain physical models. Applying shape constraints to the optimization problems above would amount to choosing among the highly degenerate sets of control Hamiltonians that solve the generic OCT problem.

Finally, we note that universal quantum computation requires nonlinear symplectic gates corresponding to the ability to count photons in the electromagnetic field [37]. The implementation of nonlinear symplectic gates necessary to achieve universal continuous quantum computation is known to be difficult to achieve with high fidelity [21]. Purification protocols are necessary to distill from an initial supply of noisy nonlinear symplectic states a smaller number of such states with higher fidelity. Future work should consider the challenges inherent in implementing such gates through the methodology of optimal control theory.

ACKNOWLEDGMENT

The authors acknowledge support from DARPA and NSF.

[1] A. P. Peirce, M. A. Dahleh, and H. Rabitz, Phys. Rev. A **37**, 4950 (1988).

[2] M. Shapiro and P. Brumer, Phys. Rep. **425**, 195 (2006).

[3] J. P. Palao and R. Kosloff, Phys. Rev. Lett. **89**, 188301 (2002).

[4] C. Tesch, L. Kurtz, and R. de Vivie-Riedle, Chem. Phys. Lett. **343**, 633 (2001).

[5] M. Grace, C. Brif, H. Rabitz, I. Walmsley, R. Kosut, and D. Lidar, J. Phys. B **40**, S103 (2007).

[6] N. Khaneja and S. J. Glaser, Chem. Phys. **267**, 11 (2001).

[7] N. Khaneja, R. Brockett, and S. J. Glaser, Phys. Rev. A **63**, 032308 (2001).

[8] P. Benioff, Int. J. Theor. Phys. **21**, 177 (1982).

[9] R. Feynman, Optics News **11**, 11 (1985).

[10] M. Nielsen and I. Chuang, *Quantum Computation and Quantum Information* (Cambridge University Press, Cambridge, England, 2000).

[11] S. Lloyd and S. L. Braunstein, Phys. Rev. Lett. **82**, 1784 (1999).

[12] P. W. Shor, Phys. Rev. A **52**, R2493 (1995).

[13] S. Braunstein, Science **282**, 705 (1998).

[14] S. D. Bartlett, B. C. Sanders, S. L. Braunstein, and K. Nemoto, Phys. Rev. Lett. **88**, 097904 (2002).

[15] S. Braunstein and A. Pati, *Quantum Information with Continuous Variables* (Kluwer, Dordrecht, 2003).

[16] M. Zhao and S. Rice, J. Chem. Phys. **95**, 2465 (1991).

[17] M. Shapiro and P. Brumer, Phys. Rep. **425**, 195 (2006).

[18] S. L. Braunstein, Phys. Rev. A **71**, 055801 (2005).

[19] H. Rabitz, M. Hsieh, and C. Rosenthal, Phys. Rev. A **72**, 052337 (2005).

[20] V. Arnold, *Mathematical Methods of Classical Mechanics, Graduate Texts in Mathematics* (Springer-Verlag, New York, 1989), Vol. 60.

[21] D. Gottesman, A. Kitaev, and J. Preskill, Phys. Rev. A **64**, 012310 (2001).

[22] V. Belavkin, Autom. Remote Control (Engl. Transl.) **44**, 178 (1983).

[23] J. Beumee and H. Rabitz, J. Math. Phys. **31**, 1253 (1990).

[24] J. Fiurasek, Phys. Rev. A **68**, 022304 (2003).

[25] B. Kraus, K. Hammerer, G. Giedke, and J. I. Cirac, Phys. Rev. A **67**, 042314 (2003).

[26] M. Paternostro, M. S. Kim, and P. L. Knight, Phys. Rev. A **71**, 022311 (2005).

[27] G. X. Li, H. T. Tan, S. P. Wu, and G. M. Huang, Phys. Rev. A **74**, 025801 (2006).

[28] A. S. Parkins, E. Solano, and J. I. Cirac, Phys. Rev. Lett. **96**, 053602 (2006).

[29] V. Jurdjevic and H. Sussmann, J. Diff. Eqns. **12**, 313 (1972).

[30] V. Jurdjevic, *Geometric Control Theory* (Cambridge University Press, Cambridge, England, 1997).

[31] A. Rothman, T. S. Ho, and H. Rabitz, Phys. Rev. A **72**, 023416

(2005).

[32] W. Press, S. Teukolsky, W. Vetterling, and B. Flannery, *Numerical Recipes in C++* (Cambridge University Press, Cambridge, England, 2002).

[33] R. Stengel, *Optimal Control and Estimation* (Dover, New York, 1994).

[34] R. Chakrabarti and H. Rabitz, Int. Rev. Phys. Chem. **26**, 671 (2007).

[35] R. Wu, R. Chakrabarti, and H. Rabitz, e-print arXiv:0708.3822 [quant-ph].

[36] See EPAPS Document No. E-PLRAAN-77-200804 for the critical topology analysis on symplectic groups. For more information on EPAPS, see http://www.aip.org/pubservs/epaps.html.

[37] S. Lloyd and E. Jean-Jacques Slotine, Phys. Rev. Lett. **80**, 4088 (1998).

[38] In both cases, local controls are generally associated with optimal fields whose Fourier spectra bear no simple relationship to system transition frequencies.